

# An Artificial Oxygenase Built from Scratch: Substrate Binding Site Identified Using a Docking Approach\*\*

Charlène Esmieu, Mickaël V. Cherrier, Patricia Amara, Elodie Girgenti, Caroline Marchi-Delapierre, Frédéric Oddon, Marina Iannello, Adeline Jorge-Robin, Christine Cavazza,\* and Stéphane Ménage\*

The need for sustainable chemistry urges the scientific community to design clean chemical processes. In this context, the concept of green chemistry has emerged,<sup>[1]</sup> and involves twelve principles with respect to avoiding both the use and the generation of hazardous substances. Biocatalysis is a promising strategy which fulfills most of these principles (catalysis, reduction of organic solvent, nondangerous synthesis and selective reactions, atom economy, nontoxic metals, etc.).<sup>[2]</sup> One approach to creating new biocatalysts for a defined reaction is the design of artificial metalloenzymes which are based on the combination of metal-based catalysis (by an inorganic complex) and protein-driven reaction selectivity, thus conferring unnatural activities to biomolecules.<sup>[3]</sup> Compared to natural enzymes, the advantage of these hybrids resides in an additional degree of optimization based on structural modifications of the inorganic complex embedded within the protein. A great variety of reactions has been tackled using artificial metalloenzymes.<sup>[5]</sup> Among them, the field of oxidation seems to be promising because artificial hybrids can overcome the drawbacks of di(mono)oxygenases, that is, the requirement of multiprotein complexes, including the redox partner (ferredoxins or NADPH reductase for example).<sup>[6]</sup>

The catalytic efficiency of an enzyme depends on an accurate combination of the catalytic site, the substrate-binding site, and the protein scaffold. This efficiency relies on

the fine control at the active site, through constraints imposed by the protein environment, on the sequence of the chemical steps and the orientation of the substrates along the catalytic cycle. Herein we report an original method for the design of an artificial monooxygenase by taking charge of the three essential parameters for enzymatic activity, with special attention to the substrate binding mode. First, we inserted inorganic catalysts into the periplasmic nickel-binding protein NikA, through supramolecular interactions, to convert it from a transport protein into a metalloenzyme.<sup>[7]</sup> Here, we have taken advantage of NikA's ability to bind iron complexes with  $N_2Py_2$  ligands,<sup>[7,8]</sup> complexes which are known catalysts for C–H, C=C, and C–OH oxidations as well as oxygen transfer to sulfides.<sup>[9]</sup> Second, molecular docking calculations have been conducted to screen sulfides for catalytic oxidation by a series of iron complex–NikA hybrids. A set of six potential substrates having a common motif was synthesized and the catalytic properties of each hybrid were determined to validate the docking simulations. Herein, we describe the proof-of-concept of our method by designing a substrate family, thus allowing us to define a new kind of artificial oxygenase for sulfoxidation.

In addition to Fe/EDTA–NikA,<sup>[7]</sup> four different hybrids were used in this study: Fe/L1–NikA, Fe/L2–NikA, Fe/L3–NikA, and Fe/L4–NikA (Figure 1). The Fe/L (L = ligand) complexes,<sup>[10]</sup> the resulting hybrids, and the crystal structures of Fe/EDTA–NikA, Fe/L3–NikA, and Fe/L4–NikA were previously described.<sup>[7,8]</sup>

The crystal structure of Fe/L1–NikA was solved at 1.7 Å resolution (PDB code ID: 4I9D, see Figure S1 and Table S1 in the Supporting Information). As previously observed for all NikA-based hybrids, Fe/L1 binds to NikA through a salt bridge between Arg137 and the carboxylate moiety of the ligand. In addition, Trp100 and Trp398 are involved in CH– $\pi$

[\*] C. Esmieu, Dr. E. Girgenti, Dr. C. Marchi-Delapierre, Dr. F. Oddon, A. Jorge-Robin, Dr. S. Ménage

Laboratoire Chimie et Biologie des Métaux, Université Joseph Fourier-Grenoble 1, CEA, DSV/IRTSV, LCBM, CNRS, UMR5249 38041 Grenoble (France)

E-mail: stephane.menage@cea.fr

Homepage: <http://www-dsv.cea.fr/irtsv/lcbm/bioce>

Dr. M. V. Cherrier, Dr. P. Amara, M. Iannello, Dr. C. Cavazza  
Metalloproteins Unit, Institut de Biologie Structurale Jean-Pierre Ebel, CEA, CNRS UMR 5075, Université Joseph Fourier-Grenoble 1 41 rue Horowitz, 38027 Grenoble Cedex 1 (France)

E-mail: christine.cavazza@ibs.fr

[\*\*] The authors are grateful to the ANR "Programme Labex" (ARCANE project n° ANR-11-LABX-003) for funding and for an ANR 08-CP2D-12 grant. We also thank the CEA, the University of Joseph Fourier, and the CNRS for institutional support, and Region Rhône-Alpes for a CIBLE grant. We also thank the staff from the ID23-eh1 beamline of the European Synchrotron Radiation Facility in Grenoble, France. We appreciate the help from the staff at the computing facilities of the CEA (DSV/GIPSI and CCRT).

Supporting information for this article is available on the WWW under <http://dx.doi.org/10.1002/anie.201209021>.

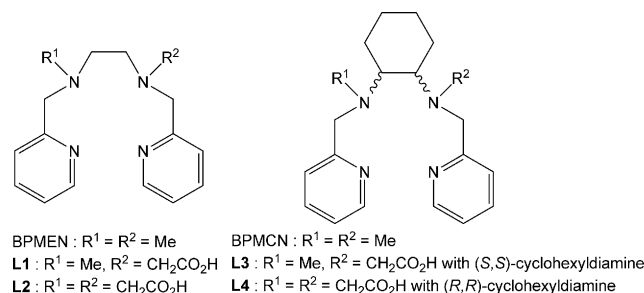


Figure 1. Selected ligands for hybrid synthesis.

interactions with different parts of the complex, and in  $\pi$ -stacking interactions with pyridine rings. As expected, two different molecules (A and B) are present in the asymmetric unit. In the case of Fe/**L3**⊂NikA and Fe/**L4**⊂NikA, the iron complexes are present with *cis*- $\beta$  and *trans* topologies in molecules A and B, respectively.<sup>[8]</sup> For Fe/**L1**⊂NikA, the electron density was much more difficult to explain because we observed a mixture of different topologies in both molecules of the asymmetric unit. Such an outcome is probably due to the absence of the cyclohexyl ring in **L1**, thus leading to the loss of multiple CH– $\pi$  interactions with tryptophan residues, compared those of Fe/**L3**. This structural difference also results in a rotation of Fe/**L1** of about 80° around the axis formed by the carboxylate moiety and the iron.

We decided to use molecular docking to find potential substrates for NikA, substrates which could bind close to the inserted catalyst (see Figure S2 in the Supporting Information). The crystal structure of Fe/**L1**<sub>trans</sub>⊂NikA was used and molecules containing a C<sub>6</sub>H<sub>5</sub>-S-CH<sub>2</sub>-X motif were extracted from the Zinc Database.<sup>[11]</sup> The main criterion was the distance between Fe of the complex and S of the molecule, a distance which was in accord with the suggested Fe–O–S transition state (see the Supporting Information for details). The results led to a set of 374 molecules, from which a family with a R<sup>1</sup>-S-CH<sub>2</sub>-CONH-R<sup>2</sup> motif (S- and N-substituted thioglycolamide; R<sup>1</sup> and R<sup>2</sup> are aromatic substituents) was identified, the simplest member being **S0** (R<sup>1</sup> = 3-NH<sub>2</sub>Ph, R<sup>2</sup> =  $\alpha$ -naphthyl). Interestingly, the skeleton of the defined substrate is comparable to the one of omeprazole or modafinil, which are major drugs from the pharmaceutical industry. **S0** is stabilized in the cavity of Fe/**L1**<sub>trans</sub>⊂NikA through a hydrogen bond between the aromatic amide function and the Gln385 side chain (Figure 2). An additional interaction was detected with Glu247.

A set of molecules, namely **S1**–**S6**, was designed based on the following criteria: the steric bulk of R<sup>1</sup> and R<sup>2</sup>, their facile synthesis, and their expected solubility in aqueous medium (**S0** was excluded because of its high insolubility; Figure 3). In the first series, **S1**–**S4**, the amino substituent of R<sup>1</sup> was replaced by various bulky substituents and R<sup>2</sup> was an aromatic ring so as to maintain the interaction between the

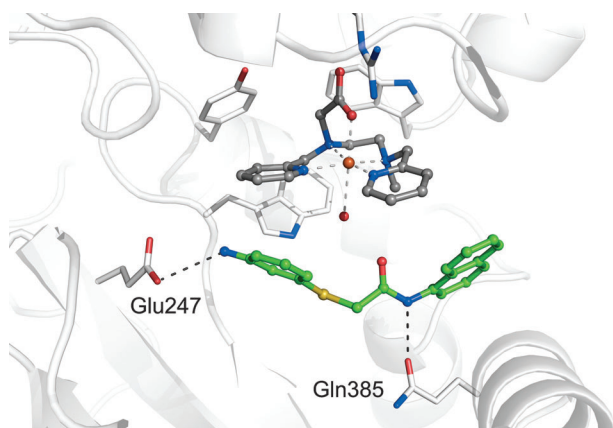
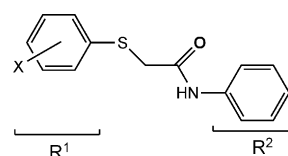


Figure 2. **S0** docked in Fe/**L1**<sub>trans</sub>⊂NikA.



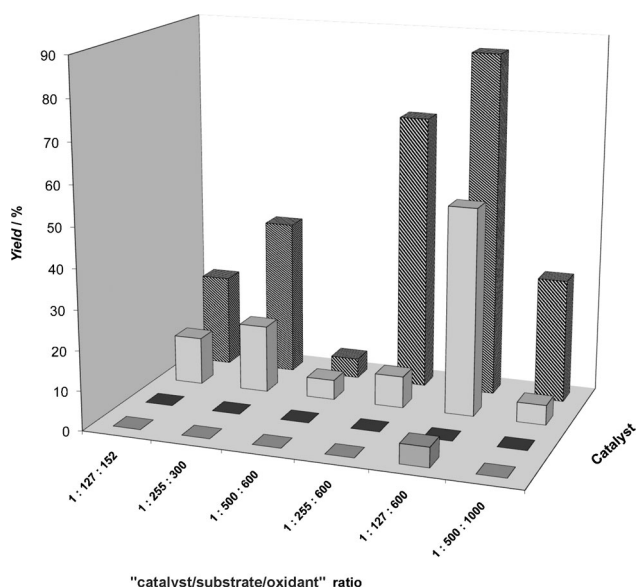
- S0** : R<sup>1</sup> = 3-NH<sub>2</sub>C<sub>6</sub>H<sub>4</sub>, R<sup>2</sup> =  $\alpha$ -naphthyl  
**S1** : R<sup>1</sup> = 4-AcNHC<sub>6</sub>H<sub>4</sub>, R<sup>2</sup> = Ph  
**S2** : R<sup>1</sup> = 4-CH<sub>3</sub>C<sub>6</sub>H<sub>4</sub>, R<sup>2</sup> = Ph  
**S3** : R<sup>1</sup> = 2,5-(MeO)<sub>2</sub>C<sub>6</sub>H<sub>4</sub>, R<sup>2</sup> = Ph  
**S4** : R<sup>1</sup> = 3,4-(MeO)<sub>2</sub>C<sub>6</sub>H<sub>4</sub>, R<sup>2</sup> = Ph  
**S5** : R<sup>1</sup> = 2,5-(MeO)<sub>2</sub>C<sub>6</sub>H<sub>4</sub>, R<sup>2</sup> = H  
**S6** : R<sup>1</sup> = 3,4-(MeO)<sub>2</sub>C<sub>6</sub>H<sub>4</sub>, R<sup>2</sup> = H  
Omeprazole\* : R<sup>1</sup> =  $\beta$ -MeO-benzimidazole and replace  
CONHR<sup>2</sup> by 4-MeO-3,5-dimethylpyridin-2-yl  
Modafinil\* : R<sup>1</sup> = (Ph)<sub>2</sub>CH, R<sup>2</sup> = H

Figure 3. Selected sulfides for iron/hybrid sulfoxidation. (\*) corresponds to the sulfide precursor of the drug.

amide group and Gln385. Conversely, **S5** and **S6** were chosen to test the influence of the absence of the R<sup>2</sup> ring on the binding mode. These six molecules were docked in Fe/**L1**<sub>trans</sub>⊂NikA: **S1**–**S4** exhibited similar interactions with the protein. Compared to **S0**, the interaction with Glu247 was lost because of the replacement of the NH<sub>2</sub> group on the aromatic ring of R<sup>1</sup>. However, their binding modes were not affected and a favorable Fe–S distance was preserved. For **S5**, the five best docking modes were found at a site that was different to that for **S1**–**S4**, and **S6** was docked at three different regions of the cavity (see Figure S3 in the Supporting Information). The influence of both the iron coordination sphere and complex topology were also tested (see Figures S4 and S5 in the Supporting Information). Molecular docking performed on Fe/**L4**<sub>trans</sub>⊂NikA showed that the presence of the second carboxylate moiety on **L4** hinders the binding of the **S1**–**S6** (Figure S5). Molecular docking was also performed for Fe/**L3**<sub>trans</sub>⊂NikA, with the same results as those obtained for Fe/**L1**<sub>trans</sub>⊂NikA. When the docking experiments were performed on Fe/**L3**<sub>cis- $\beta$</sub> ⊂NikA, only one molecule, **S1**, bound in the same cavity (Figure S4A), and **S2**–**S6** were present at a different site or with a different orientation (see the Supporting Information and Figure S4B). This observation identified **S1** a good candidate for a reference substrate in this study.

The sulfides **S1**–**S6** were synthesized by a nucleophilic attack of the chosen substituted aromatic sulfide anion on the 2-chloro-*N*-phenylacetamide. The corresponding products, that is, sulfoxides and sulfones, were obtained by direct oxidation using NaIO<sub>4</sub> and KHSO<sub>5</sub>/wet montmorillonite, respectively.<sup>[12]</sup> Under these reaction conditions, a mixture of the sulfone and sulfoxide products was always obtained, thus leading, after purification, to a (46  $\pm$  5) % yield of sulfoxide and (56  $\pm$  5) % yield of the corresponding sulfone in the case of **S1**. Interestingly, all previously reported procedures also reported product mixtures (please follow our correction).

Initially, Fe/**L1**⊂NikA was tested for the catalytic oxidation of **S1** by NaOCl (see Figure S6 in the Supporting Information). We also tried other oxidants such as dioxygen or H<sub>2</sub>O<sub>2</sub> but no activity could be detected. The experimental



**Figure 4.** Yield of sulfoxide with **S1** as a substrate depending on the catalytic conditions: gray: NaOCl, black: NaOCl + Fe/**L1**, light gray: NaOCl + NikA, solid black: NaOCl + Fe/**L1**:NikA, Catalyst: 5 nmol, 37  $\mu$ M in 10 mM HEPES, pH 7.0, stirring at room temperature, 4 h.

conditions were optimized to determine the catalytic properties of the hybrid by varying the catalyst/substrate/oxidant ratio (Figure 4). The free inorganic Fe/**L1** complex was totally inactive under each of the reaction conditions tested (see the Supporting Information), whereas either NikA alone or **L1**:NikA catalyzed a low production of sulfoxide. In addition, a minor by-product, identified as the dichlorinated sulfoxide 4-AcNH-C<sub>6</sub>H<sub>5</sub>-SO-C(Cl)<sub>2</sub>-CO-NH-C<sub>6</sub>H<sub>5</sub> (see Figure S7 in the Supporting Information) was observed. However, this product resulted from an uncatalyzed reaction, because a higher yield (17%) was obtained in the absence of any component of the hybrid and with a large excess of NaOCl. In all cases, the overoxidation product (sulfone) was never detected. Only the hybrid catalyzed the exclusive formation of the sulfoxide with good yields after four hours (up to 86%, Figure 4). However, variations of the substrate/oxidant ratio drastically affected the yield of the reaction. On one hand, as expected, increasing the oxidant concentration led to a better yield for a given substrate concentration. For example, by changing the catalyst/substrate/oxidant ratio from 1:255:300 to 1:255:600, the reaction yield increased from (45  $\pm$  5) to (69  $\pm$  5)%. On the other hand, if the substrate concentration increased for a given oxidant concentration, the yield of the sulfoxide decreased. For instance in the case of an amount of 600 equivalents of NaOCl, the yield decreased from 86 to 68%, then to 5% for a substrate amount increasing from 127 to 255 then 500 equivalents, respectively. The optimal reaction conditions (1:250:600) provided a high catalytic efficiency. Under these reaction conditions, (79  $\pm$  5)% of the total amount of **S1** was consumed in 4 hours and a TON of 173 with a TOF of 43 h<sup>-1</sup> were measured, with a sulfoxide yield of (69  $\pm$  5)%. So far, our enzyme displays one of the higher TONs for sulfide oxidation catalyzed by an artificial metalloenzyme.<sup>[6c-f]</sup>

The three other Fe/**L3**:NikA and Fe/**EDTA**:NikA hybrids were then tested for their ability to selectively oxidize **S1**. Only Fe/**L3**:NikA was able to provide a high yield and selectivity comparable to those of Fe/**L1**:NikA (64% versus 69% for the yield and 163 versus 173 for the TON), and Fe/**EDTA**:NikA, Fe/**L2**:NikA, and Fe/**L4**:NikA were found to be inactive (see Table S2 in the Supporting Information). On one hand, the absence of activity for Fe/**EDTA**:NikA attests to the fact that the metal ion is not sufficient to gain sulfide oxidation but that the first coordination sphere, that is the ligand providing a N<sub>4</sub>O<sub>2</sub> coordination to the iron, is essential for tuning its electronic properties. On the other hand, the difference in activity between the different Fe/**L**:NikA complexes correlates to the presence of a labile site in the iron coordination sphere and was confirmed by structural analyses (see Figure S1 in the Supporting Information).<sup>[8]</sup> Compared to Fe/**L2**:NikA and Fe/**L4**:NikA, Fe/**L1**:NikA and Fe/**L3**:NikA, which are missing one carboxylate moiety of the ligand, contain a water molecule to complete the coordination sphere, thus leading to an open-shell coordination. Consequently, the Lewis acidity of the iron should be increased, thereby reinforcing its ability to activate the oxidant (NaOCl) by direct binding to the metal center.<sup>[13]</sup> Finally, the initial oxidation rates of the two efficient hybrids, Fe/**L1**:NikA and Fe/**L3**:NikA, are distinct and attest to the fact that the nature of the ligand affects the kinetics of the sulfoxidation reaction. This data additionally supports the proposal that the oxygen-transfer reaction is centered on the iron complex (see Figure S8 in the Supporting Information).

The substrate analogues **S2–S6** (Figure 3) were tested with Fe/**L1**:NikA. They were all oxidized to produce the corresponding sulfoxides to a certain extent (Table 1). Indeed, the sulfoxide yields were dependent on the steric hindrance of the substrate. The most bulky substrates, **S3** and **S4**, having the dimethoxyphenyl groups as R1, gave yields of only 40 and 18%, respectively. In contrast, **S2** which has a methylphenyl group as R1, led to an increased yield of 78%. The selectivity for **S1–S3** was complete but in case of **S4** it fell to the same level as that of the uncatalyzed reaction (18%). Interestingly, sulfoxides were produced when the corresponding substrates were shown by molecular docking to be oriented in front of the embedded iron complex. However, the case of **S4** is puzzling because it docks in the required position but displays low reactivity. We suggest a lower affinity of the hybrid for **S4** in solution. The difference in nucleophilicity of the sulfur atom would be minimal between **S3** and **S4** and cannot be responsible for the difference in reactivity. Therefore, the difference would arise from a subtle combination of steric effects and hydrophobicity which allow the formation of supramolecular interactions between the protein and the molecule. Such interactions could be favorable in the case of **S1–S3** but disadvantageous in the case of **S4**. For **S5** and **S6**, the yield and the selectivity were found to be similar to those observed in the absence of the hybrid. Here, the absence of catalytic activity is directly related to a nonspecific binding of the molecules in the **S0** cavity, or even outside (see Figure S3 in the Supporting Information). This nonspecific binding is probably due to the smaller substrate bulk and the loss of hydrophobic interactions with the protein. In addition, the

**Table 1:** Catalytic properties of Fe/L1C NikA for the oxidation of **S1–S6** by NaOCl.<sup>[a]</sup>

Substrate	R1	R2	Hybrid	Yield [%]	Sel. [%]	TON
<b>S1</b>	4-AcNHC <sub>6</sub> H <sub>4</sub>	Ph	no yes	0 69	0 87 <sup>[b]</sup>	– 173
<b>S2</b>	4-CH <sub>3</sub> C <sub>6</sub> H <sub>4</sub>	Ph	no yes	10 78	100 100	– 199
<b>S3</b>	2,5-(MeO) <sub>2</sub> C <sub>6</sub> H <sub>3</sub>	Ph	no yes	14 40	20 <sup>[b]</sup> 100	– 102
<b>S4</b>	3,4-(MeO) <sub>2</sub> C <sub>6</sub> H <sub>3</sub>	Ph	no yes	15 18	2 18 <sup>[b]</sup>	– 46
<b>S5</b>	2,5-(MeO) <sub>2</sub> C <sub>6</sub> H <sub>3</sub>	H	no yes	12 15	12 15	– –
<b>S6</b>	3,4-(MeO) <sub>2</sub> C <sub>6</sub> H <sub>3</sub>	H	no yes	85 62	85 62	– –

[a] Catalytic conditions: 10 mM HEPES buffer, pH 7.0, Fe-L1C NikA (5 nmol, 37  $\mu$ M), catalyst/substrate/NaOCl = 1:255:600, stirring at room temperature for 4 h. Errors were estimated to be about 5% from three different runs. [b] A dichlorinated by-product was observed.

high solubility observed for **S5** and **S6** compared to that for **S1–S4** supports our interpretation, thus indicating that it would be directly attacked in solution by the oxidant to generate the dichlorinated by-product.<sup>[14]</sup>

Thus, we have designed a reference substrate for our artificial enzyme, and it contains the Ph-S-CH<sub>2</sub>-CONH-Ph motif. We have also demonstrated that the chemoselectivity is driven by supramolecular interactions between the protein and the substrate at a position close to the catalytic center, thus validating our docking approach. However, this outcome is essential but not sufficient for enantioselectivity as in our hands only weak, but measurable *ee* values were detected (10% for **S1**, and 5% for **S2** and **S3**). This data underlines the importance of the protein scaffold on the enantioselective control of a reaction. Protein and complex modifications should be undertaken to optimize the enantioselective control.

Through this work, we have implemented an original method to design a selective oxygenase for sulfide oxidation and highlighted the synergetic effect of each partner. The docking method allowed identification of a substrate binding site in a non-enzymatic NikA and selection of a proper substrate. This work is another example of the power of synthetic biology, wherein a natural system is redirected to broader applications for sustainable chemistry.

Received: November 11, 2012

Published online: February 25, 2013

**Keywords:** computational chemistry · iron · metalloenzymes · oxidation · sulfur

- [1] C. J. Li, P. T. Anastas, *Chem. Soc. Rev.* **2012**, *41*, 1413–1414.
- [2] a) C. M. Clouthier, J. N. Pelletier, *Chem. Soc. Rev.* **2012**, *41*, 1585–1605; b) S. Enthaler, K. Junge, M. Beller, *Angew. Chem.* **2008**, *120*, 3363–3367; *Angew. Chem. Int. Ed.* **2008**, *47*, 3317–3321.
- [3] a) F. Rosati, G. Roelfes, *ChemCatChem* **2010**, *2*, 916–927; b) M. R. Ringenberg, T. R. Ward, *Chem. Commun.* **2011**, *47*, 8470–8476; c) M. T. Reetz, *Angew. Chem.* **2011**, *123*, 144–182; *Angew. Chem. Int. Ed.* **2011**, *50*, 138–174.
- [4] a) T. Ueno, S. Abe, N. Yokoi, Y. Watanabe, *Coord. Chem. Rev.* **2007**, *251*, 2717–2731; b) J. Steinreiber, T. R. Ward, *Coord. Chem. Rev.* **2008**, *252*, 751–766; c) Y. Lu, N. Yeung, N. Sieracki, N. M. Marshall, *Nature* **2009**, *460*, 855–862; d) A. J. Boersma, R. P. Megens, B. L. Feringa, G. Roelfes, *Chem. Soc. Rev.* **2010**, *39*, 2083–2092.
- [5] a) A. J. Boersma, D. Coquiere, D. Geerdink, F. Rosati, B. L. Feringa, G. Roelfes, *Nat. Chem.* **2010**, *2*, 991–995; b) C. Mayer, D. G. Gillingham, T. R. Ward, D. Hilvert, *Chem. Commun.* **2011**, *47*, 12068–12070; c) G. Roelfes, B. L. Feringa, *Angew. Chem.* **2005**, *117*, 3294–3296; *Angew. Chem. Int. Ed.* **2005**, *44*, 3230–3232; d) P. Fournier, R. Fiammengio, A. Jaschke, *Angew. Chem.* **2009**, *121*, 4490–4493; *Angew. Chem. Int. Ed.* **2009**, *48*, 4426–4429; e) Q. Jing, K. Okrasa, R. J. Kazlauskas, *Chem. Eur. J.* **2009**, *15*, 1370–1376.
- [6] a) V. Köhler, J. C. Mao, T. Heinisch, A. Pordea, A. Sardo, Y. M. Wilson, L. Knorr, M. Creus, J. C. Prost, T. Schirmer, T. R. Ward, *Angew. Chem.* **2011**, *123*, 11055–11058; *Angew. Chem. Int. Ed.* **2011**, *50*, 10863–10866; b) M. Allard, C. Dupont, V. M. Robles, N. Doucet, A. Lledos, J. D. Maréchal, A. Urvoas, J. P. Mahy, R. Ricoux, *ChemBioChem* **2012**, *13*, 240–251; c) M. Ohashi, T. Koshiyama, T. Ueno, M. Yanase, H. Fujii, Y. Watanabe, *Angew. Chem.* **2003**, *115*, 1035–1038; *Angew. Chem. Int. Ed.* **2003**, *42*, 1005–1008; d) A. Pordea, M. Creus, J. Panek, C. Duboc, D. Mathis, M. Novic, T. R. Ward, *J. Am. Chem. Soc.* **2008**, *130*, 8085–8088; e) P. Rousselot-Pailley, C. Bochot, C. Marchi-Delapierre, A. Jorge-Robin, L. Martin, J. C. Fontecilla-Camps, C. Cavazza, S. Ménage, *ChemBioChem* **2009**, *10*, 545–552; f) J. R. Carey, S. K. Ma, T. D. Pfister, D. K. Garner, H. K. Kim, J. A. Abramite, Z. L. Wang, Z. J. Guo, Y. Lu, *J. Am. Chem. Soc.* **2004**, *126*, 10812–10813.
- [7] M. V. Cherrier, L. Martin, C. Cavazza, L. Jacquamet, D. Lemaire, J. Gaillard, J. C. Fontecilla-Camps, *J. Am. Chem. Soc.* **2005**, *127*, 10075–10082.
- [8] M. Cherrier, E. Girgenti, P. Amara, M. Iannello, C. Marchi-Delapierre, J. C. Fontecilla-Camps, S. Ménage, C. Cavazza, *J. Biol. Inorg. Chem.* **2012**, *17*, 817–829.
- [9] a) E. P. Talsi, K. P. Bryliakov, *Coord. Chem. Rev.* **2012**, *256*, 1418–1434; b) L. Que, W. B. Tolman, *Nature* **2008**, *455*, 333–340; c) K. Schroder, K. Junge, B. Bitterlich, M. Beller in *Iron Catalysis: Fundamentals and Applications*; Vol. 33 (Ed.: B. Plietker), Springer, Berlin, **2011**, pp. 83–109.
- [10] F. Oddon, E. Girgenti, C. Lebrun, C. Marchi-Delapierre, J. Pécaut, S. Ménage, *Eur. J. Inorg. Chem.* **2012**, 85–96.
- [11] J. J. Irwin, B. K. Shoichet, *J. Chem. Inf. Model.* **2005**, *45*, 177–182.
- [12] a) T. Sato, Y. Wada, M. Nishimoto, H. Ishibashi, M. Ikeda, *J. Chem. Soc. Perkin Trans. 1* **1989**, 879–886; b) M. Hirano, J. Tomaru, T. Morimoto, *Bull. Chem. Soc. Jpn.* **1991**, *64*, 3752–3754.
- [13] a) Y. Mekmouche, S. Ménage, J. Pécaut, C. Lebrun, L. Reilly, V. Schuenemann, A. Trautwein, M. Fontecave, *Eur. J. Inorg. Chem.* **2004**, 3163–3171; b) Y. Feng, J. England, L. Que, *ACS Catal.* **2011**, *1*, 1035–1042.
- [14] M. Deborde, U. von Gunten, *Water Res.* **2008**, *42*, 13–51.